

SCIENTIFIC REPORTS



OPEN

Function of capric acid in cyclophosphamide-induced intestinal inflammation, oxidative stress, and barrier function in pigs

Sang In Lee¹ & Kyung Soo Kang²

The small intestine is not only critical for nutrient absorption, but also serves as an important immune organ. Medium-chain fatty acids have nutritional and metabolic effects and support the integrity of the intestinal epithelium. However, their roles in intestinal immunity in pigs are not fully understood. We investigated the effects of a medium-chain fatty acid, capric acid, on intestinal oxidative stress, inflammation, and barrier function in porcine epithelial cells and miniature pigs after treatment with the immune suppressant cyclophosphamide. Capric acid alleviated inflammatory cytokine production (TNF- α and IL-6) and related gene expression (*NF- κ B*, *TNF- α* , *IFN- γ*), alleviated oxidative stress (GSSG/GSH ratio, H₂O₂, and malondialdehyde), and increased oxidative stress-related gene expression (*SOD1* and *GCLC*) in cyclophosphamide-treated IPEC-J2 cells. The permeability of FD-4 and expression of *ZO-1* and *OCLN* in cyclophosphamide-treated IPEC-J2 cells were reduced by capric acid. Dietary capric acid reduced TNF- α , IL-6, and MDA levels and increased SOD, GPx, and the expression of genes related to pro-inflammatory, oxidative stress, and intestinal barrier functions in cyclophosphamide-treated miniature pigs. These results revealed that capric acid has protective effects against cyclophosphamide-induced small intestinal dysfunction in pigs.

The gastrointestinal (GI) tract is not only important for the digestion, absorption, and metabolism of nutrients, but also serves as a critical immune organ, since it has the most immune cells in the body¹. Pathogenic or nonpathogenic challenges activate the GI immune system, leading the production of a diverse set of specialised cells and signalling molecules, especially pro-inflammatory cytokines, such as tumour necrosis factor (TNF)- α , interleukin (IL)-1 β , and IL-6, resulting in intestinal mucosal injury and dysfunction via the over-production of these cytokines^{2,3}. In pigs, intestinal infections drastically amplify inflammatory responses, affecting the intestinal morphology, mucosal functions (including nutrient digestion and absorption), and intestinal barrier function, resulting in reduced feed intake, weight gain, and an altered gain/feed ratio⁴⁻⁷. In addition to intestinal pathogenic infection, intestinal inflammation can be induced by stress, such as weaning and oxidative stress^{3,8}.

Oxidative stress caused by an imbalance between pro-oxidants and anti-oxidants is associated with the excessive production of reactive oxygen species (ROS) and an antioxidant deficiency⁹. In the small intestinal epithelium, oxidative stress is a major cause of barrier malfunction and the pathogenesis of various gastrointestinal diseases, such as enterocolitis, gastrointestinal cancers, celiac disease, and inflammatory bowel disease¹⁰⁻¹². The small intestinal epithelium serves as an important part of the first line of defence against pathogens and regulates the absorption of solutes and macromolecules, including nutrients. The intestinal barrier is composed of a single layer of columnar epithelial cells sealed by junctional complexes including, tight and adherens junctions, in close proximity to the apical and lateral side of the paracellular space. These structures are affected by oxidative stress, since the pathophysiology of a redox imbalance is characterised by disrupted junctional complexes¹³⁻¹⁵. Disruption of the junctional complexes can facilitate the passage of macromolecules and pathogens through the intestinal epithelium into the body¹⁶⁻¹⁸. Oxidative stress also affects mitosis, apoptosis, and differentiation in small intestinal epithelial cells from the crypt to the villus.

¹Department of Animal Resource and Science, Dankook University, Cheonan, Chungnam, 330-714, Republic of Korea. ²Bio Division, Medikinetics, Inc., Hansan-gil, Pyeongtaek-si, Gyeonggi-do, 17792, Republic of Korea. Correspondence and requests for materials should be addressed to K.S.K. (email: kks@spf-pig.com)

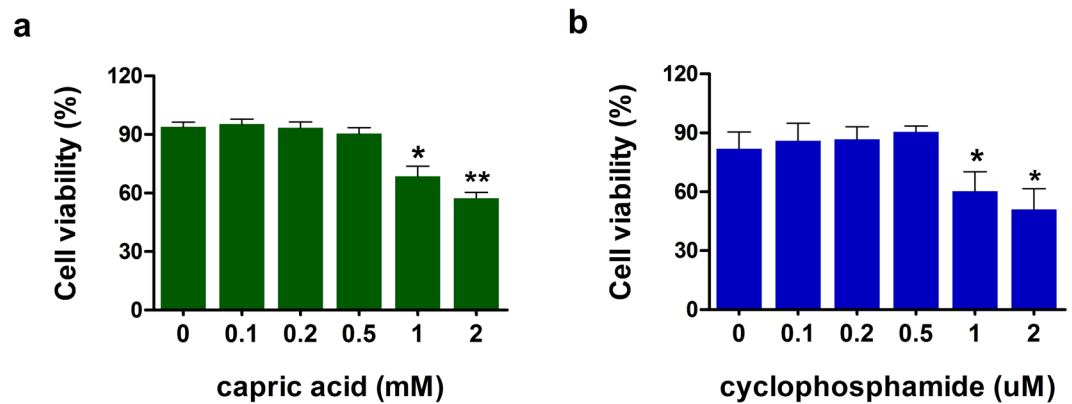


Figure 1. Cytotoxicity of capric acid and cyclophosphamide in IPEC-J2 cells. Cell viability was determined by MTT assays. (a) IPEC-J2 cells were incubated with capric acid (0–2 mM) for 24 h. (b) IPEC-J2 cells were incubated with cyclophosphamide (0–2 μM) for 1 h. Error bars indicate the standard error of the mean ($n = 3$). Significant differences between control and treatment groups are indicated as ** $p < 0.01$ and * $p < 0.05$.

Fatty acids, used as feed additives, are important components of the cell membrane, cell-signalling molecules, metabolic substrates in many biochemical pathways, and immune modulators¹⁹. Medium-chain fatty acids (MCFAs), with aliphatic tails of six to twelve carbon atoms, have specific nutritional and metabolic effects, including rapid digestion, passive absorption, and obligatory oxidation^{8,20}. MCFAs also support the integrity of the intestine, increasing the length of villi and reducing the crypt depth in the small intestine^{21–23}. In addition, studies on the effects of various MCFAs such as capric acid and caprylic acid, on the intestinal epithelium and inflammation have indicated that these MCFAs have roles or effects^{24,25}. However, little is known about the impact of capric acid, an MCFA, on the physiological function of the small intestine in pigs. Therefore, it is important to study the effect of individual MCFAs, such as capric acid, on the intestinal epithelium and the integrity of the intestine. In the present study, we investigated the functions of capric acid in small intestinal epithelial cells after cyclophosphamide treatment in pigs. To our knowledge, this is the first study of the effect of capric acid on intestinal oxidative stress, inflammation, and barrier function in porcine epithelial cells and miniature pigs.

Results

Viability of intestinal epithelial cells after capric acid and cyclophosphamide treatment. To determine the appropriate dose of capric acid and cyclophosphamide for small intestinal epithelial cells, the viability of IPEC-J2 cells was monitored. Exposure to 1 μM CTX ($p < 0.05$) for 1 h decreased the viability of IPEC-J2 cells (Fig. 1a). Pre-treatment with 1 mM capric acid decreased the viability of IPEC-J2 cells (Fig. 1b). Based on these results, capric acid at 500 μM and cyclophosphamide at 500 μM applied for 1 h were considered safe and were used for subsequent experiments.

Effect of capric acid on inflammatory markers after cyclophosphamide treatment. The effects of capric acid on immune reactions to cyclophosphamide treatment in IPEC-J2 cells were examined. A significantly higher TNF-α concentration was observed in IPEC-J2 cells after treatment with cyclophosphamide than in controls ($p < 0.01$) (Fig. 2a). Pre-treatment with capric acid significantly reduced the TNF-α concentration after cyclophosphamide of treatment in IPEC-J2 cells ($p < 0.05$) (Fig. 2a). A significantly higher IL-6 concentration was observed in IPEC-J2 cells after cyclophosphamide treatment than in control cells ($p < 0.05$) (Fig. 2b). Pre-treatment with capric acid significantly reduced the IL-6 concentration after treatment with cyclophosphamide in IPEC-J2 cells ($p < 0.05$) (Fig. 2b).

After cyclophosphamide treatment, the relative expression levels of pro-inflammatory genes, such as *NF-κB* ($p < 0.01$), *TNF-α* ($p < 0.05$), *IFN-γ* ($p < 0.01$), and *IL-6* ($p < 0.01$) were significantly higher than the expression levels in control cells (Fig. 3a). Pre-treatment with capric acid resulted in reduced *NF-κB* ($p < 0.05$), *TNF-α* ($p < 0.05$), and *IFN-γ* ($p < 0.05$) mRNA levels after treatment with cyclophosphamide in IPEC-J2 cells (Fig. 3a). The levels of *IL-4* ($p < 0.05$) and *IL-10* ($p < 0.001$), anti-inflammation genes, were significantly higher in capric acid-treated cells than in control cells after cyclophosphamide treatment (Fig. 3b). Pre-treatment with capric acid increased the expression of *IL-4* ($p < 0.05$) and *IL-10* ($p < 0.01$) after cyclophosphamide treatment in IPEC-J2 cells (Fig. 3b).

Capric acid alleviates cyclophosphamide-induced oxidative stress in IPEC-J2 cells. The GSSG/GSH ratio in cyclophosphamide-treated IPEC-J2 cells was significantly higher than that in control cells ($p < 0.05$) (Fig. 4a). Pre-treatment with capric acid significantly reduced the GSSG/GSH ratio after cyclophosphamide treatment ($p < 0.05$) (Fig. 4a). To test whether capric acid treatment alleviates ROS production in response to cyclophosphamide-induced oxidative stress in IPEC-J2 cells, the relative extracellular H₂O₂ level was monitored (Fig. 4b). Significantly higher H₂O₂ levels were observed in IPEC-J2 cells after cyclophosphamide treatment than in control cells ($p < 0.05$) (Fig. 4b). Pre-treatment with capric acid significantly reduced the extracellular H₂O₂ level after cyclophosphamide treatment ($p < 0.05$) (Fig. 4b). Malondialdehyde levels were significantly higher in

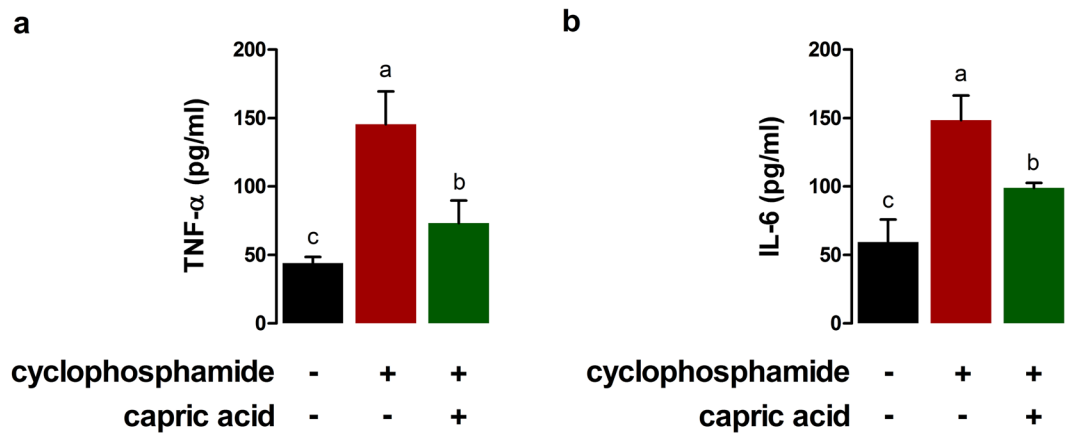


Figure 2. Effects of capric acid treatment on the production of the inflammatory cytokines (a) TNF- α and (b) IL-6 after cyclophosphamide treatment in IPEC-J2 cells. Concentrations of TNF- α and IL-6 in the cell supernatants were detected by ELISA. Mean cytokine concentrations from several independent experiments are presented ($n = 3$). Error bars indicate the standard error of the mean. A p-value of < 0.05 was considered statistically significant. Lowercase letters (a,b,c) indicate significant differences between treatments based on Duncan multiple range tests.

cyclophosphamide-treated IPEC-J2 cells than in control cells ($p < 0.01$) (Fig. 4c). Pre-treatment with capric acid significantly reduced the level of the malondialdehyde after cyclophosphamide treatment ($p < 0.05$) (Fig. 4c).

After cyclophosphamide treatment, relative expression levels of oxidative stress-related genes, such as *SOD1* ($p < 0.05$), *GCLM* ($p < 0.05$), *GCLC* ($p < 0.01$), and *CAT* ($p < 0.05$), were significantly lower compared to the expression levels in control cells (Fig. 5). Pre-treatment with capric acid significantly increased the expression of *SOD1* ($p < 0.05$) and *GCLC* ($p < 0.05$) after cyclophosphamide treatment in IPEC-J2 cells (Fig. 5).

Capric acid affects intestinal barrier function in cyclophosphamide-treated IPEC-J2 cells. To test whether capric acid treatment affects intestinal barrier function in cyclophosphamide-treated IPEC-J2 cells, the permeability of FD-4 was measured. The permeability of FD-4 in cyclophosphamide-treated IPEC-J2 cells was significantly higher than that of the control cells ($p < 0.001$) (Fig. 6a). Pre-treatment with capric acid significantly reduced the permeability of FD-4 in cyclophosphamide-treated IPEC-J2 cells ($p < 0.05$) (Fig. 5).

Next, we tested whether capric acid affects tight junction complexes on cyclophosphamide-treated IPEC-J2 cells (Fig. 6b). The mRNA expression levels of *ZO-1* and *OCN* were significantly lower in cyclophosphamide-treated IPEC-J2 cells than in control cells ($p < 0.05$) (Fig. 6b). Pre-treatment with capric acid significantly increased the expression of *ZO-1* and *OCN* in cyclophosphamide-treated IPEC-J2 cells ($p < 0.05$) (Fig. 6b).

In vivo effect of capric acid on inflammatory and oxidative stress markers in blood serum in cyclophosphamide-treated pigs. To confirm the effect of capric acid on inflammation and oxidative stress observed in cyclophosphamide-treated IPEC-J2 cells *in vitro*, the levels of inflammatory and oxidative stress markers were evaluated in blood serum in cyclophosphamide-treated pigs *in vivo*. The TNF- α concentration was significantly higher in the blood serum of cyclophosphamide-treated pigs than in control pigs ($p < 0.05$) (Fig. 7a). Dietary treatment with capric acid significantly reduced the TNF- α concentration in the blood serum in cyclophosphamide-treated pigs ($p < 0.05$) (Fig. 7a). Additionally, a significantly higher IL-6 concentration was observed in the blood serum of cyclophosphamide-treated pigs than in control pigs ($p < 0.05$) (Fig. 7b). Dietary treatment with capric acid significantly reduced the IL-6 concentration in the blood serum of cyclophosphamide-treated pigs ($p < 0.05$) (Fig. 7b).

The SOD level in the blood serum of cyclophosphamide-treated pigs was significantly lower than that of control pigs ($p < 0.05$) (Fig. 8a). Dietary treatment with capric acid significantly increased the SOD level in the blood serum of cyclophosphamide-treated pigs ($p < 0.05$) (Fig. 8a). GPx activity was significantly lower in the blood serum of cyclophosphamide-treated pigs than in control pigs ($p < 0.05$) (Fig. 8b). Dietary treatment with capric acid significantly increased the GPx activity in the blood serum of cyclophosphamide-treated pigs ($p < 0.05$) (Fig. 8b). The malondialdehyde level was significantly higher in the blood serum of cyclophosphamide-treated pigs than in control pigs ($p < 0.01$) (Fig. 8c). Dietary treatment with capric acid significantly reduced the malondialdehyde level in the blood serum of cyclophosphamide-treated pigs ($p < 0.05$) (Fig. 8c).

In vivo effects of capric acid on mRNA expression in cyclophosphamide-treated pigs. We examined the expression of mRNAs related to inflammation and oxidative stress in peripheral blood mononuclear cells and those related to intestinal barrier function in the jejunum of the small intestine in cyclophosphamide-treated pigs. The relative expression levels of pro-inflammatory genes, such as *TNF- α* ($p < 0.01$), *IFN- γ* ($p < 0.01$), *IL-6* ($p < 0.01$), and *IL-8* ($p < 0.01$) were significantly higher and those of anti-inflammatory genes, such as *IL-6* ($p < 0.05$) and *IL-8* ($p < 0.01$) were significantly lower in cyclophosphamide-treated pigs than in control pigs (Fig. 9a and b). Dietary treatment with capric acid significantly reduced the expression of *TNF- α* ($p < 0.05$), *IL-6*

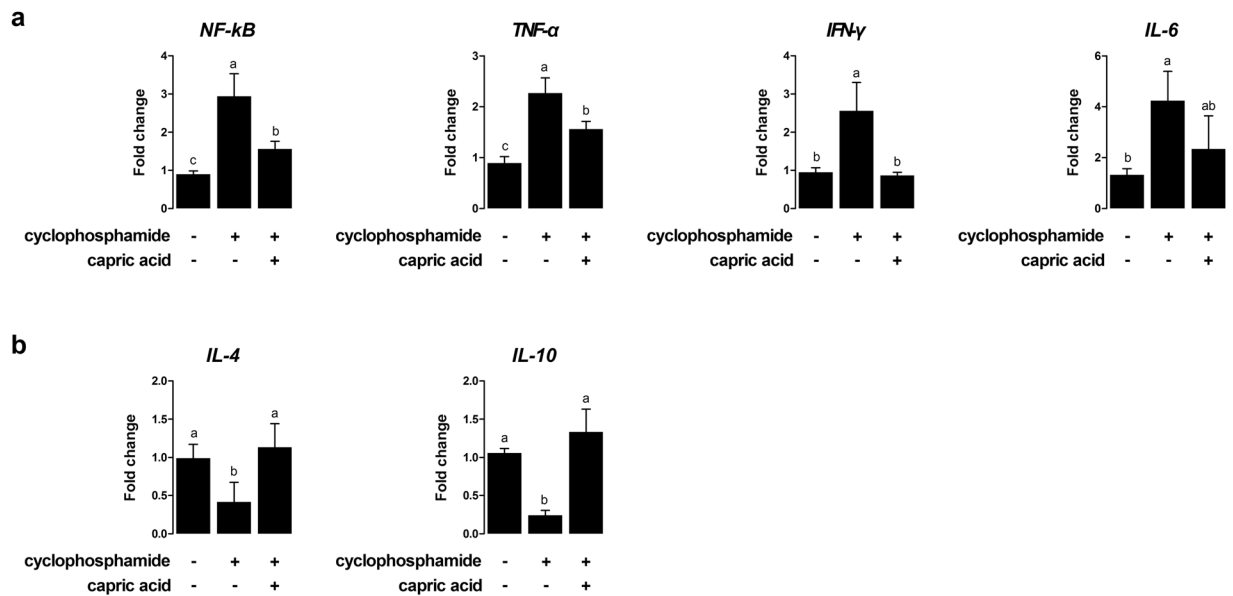


Figure 3. Relative quantitative expression of genes encoding (a) pro-inflammatory cytokines (TNF- α , IFN- γ , and IL-6) and (b) anti-inflammatory cytokines (IL-4 and IL-10) after capric acid treatment and cyclophosphamide treatment in IPEC-J2 cells. The qRT-PCR data were normalised to the expression of *GAPDH* as an endogenous control gene and calculated using the $2^{-\Delta\Delta C_t}$ method ($n = 3$). Error bars indicate the standard error of the mean. A p-value of <0.05 indicated statistical significance. Lowercase letters (a, b, c) indicate significant differences between treatments based on Duncan multiple range tests.

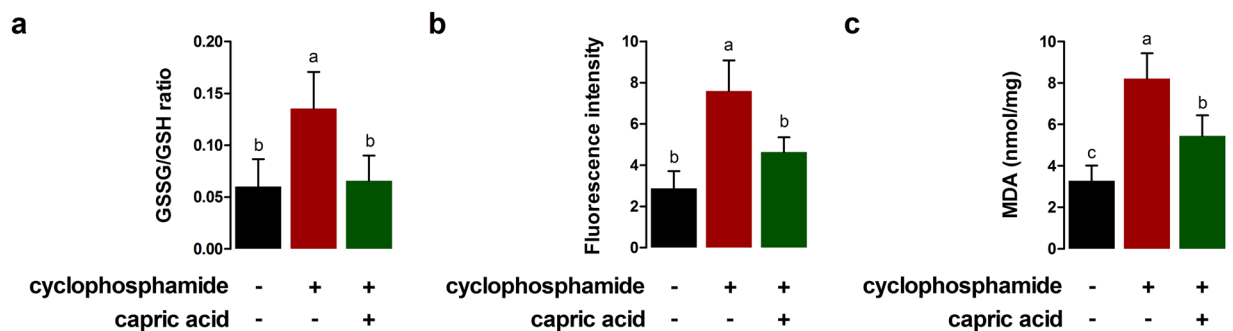


Figure 4. Effects of capric acid treatment on cyclophosphamide-induced oxidative stress in IPEC-J2 cells. (a) Glutathione (GSH) and glutathione disulphide (GSSG) concentrations were analysed. (b) Intracellular H_2O_2 levels were measured. Fluorescence was measured by the Amplex Red method. (c) the malondialdehyde (MDA) level was measured by ELISA. Error bars indicate the standard error of the mean ($n = 3$). A p-value of <0.05 was considered to indicate statistical significance. Lowercase letters (a,b,c) indicate significant differences between treatments by the Duncan multiple range tests.

($p < 0.01$), and *IL-8* ($p < 0.05$) and increased the expression of *IL-4* ($p < 0.05$) in peripheral blood mononuclear cells of cyclophosphamide-treated pigs (Fig. 9a and b).

In cyclophosphamide-treated pigs, the relative expression levels of oxidative stress-related genes, such as *SOD1* ($p < 0.05$), *GCLM* ($p < 0.05$), *GCLC* ($p < 0.01$), and *CAT* ($p < 0.01$), were significantly lower than those in control pigs (Fig. 10a). Dietary treatment with capric acid significantly increased the expression of *SOD1* ($p < 0.05$), *GCLM* ($p < 0.05$), *GCLC* ($p < 0.05$), and *CAT* ($p < 0.05$) in peripheral blood mononuclear cells of cyclophosphamide-treated pigs (Fig. 10a). The relative expression levels of intestinal barrier function-related genes, such as *ZO-1* ($p < 0.05$) and *OCN* ($p < 0.05$), were significantly lower in cyclophosphamide-treated pigs than in control pigs (Fig. 10b). Dietary treatment with capric acid significantly increased the expression of *OCN* ($p < 0.01$) in the jejunum in cyclophosphamide-treated pigs (Fig. 10b).

Discussion

We found that capric acid, an MCFA, significantly reduced the TNF- α and IL-6 concentrations after cyclophosphamide treatment in porcine intestinal epithelial cells. Fatty acids are an important energy source and improve intestinal health by inhibiting the over-release of intestinal inflammatory mediators, especially pro-inflammatory cytokines, in pigs⁸. Fatty acids could affect inflammatory cell function and inflammatory processes by a variety

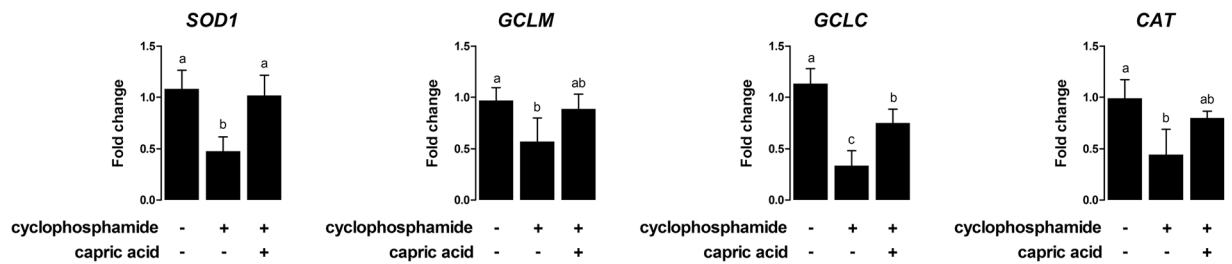


Figure 5. Relative quantitative expression of the genes encoding antioxidant enzymes (SOD1, GCLM, GCLC, and CAT) after capric acid treatment and cyclophosphamide treatment in IPEC-J2 cells. The qRT-PCR data were normalised relative to the expression of *GAPDH* as an endogenous control gene and calculated using the $2^{-\Delta\Delta C_t}$ method ($n = 3$). Error bars indicate the standard error of the mean. A p-value of <0.05 was considered to indicate statistical significance. Lowercase letters (a,b,c) indicate significant differences between treatments based on Duncan multiple range tests.

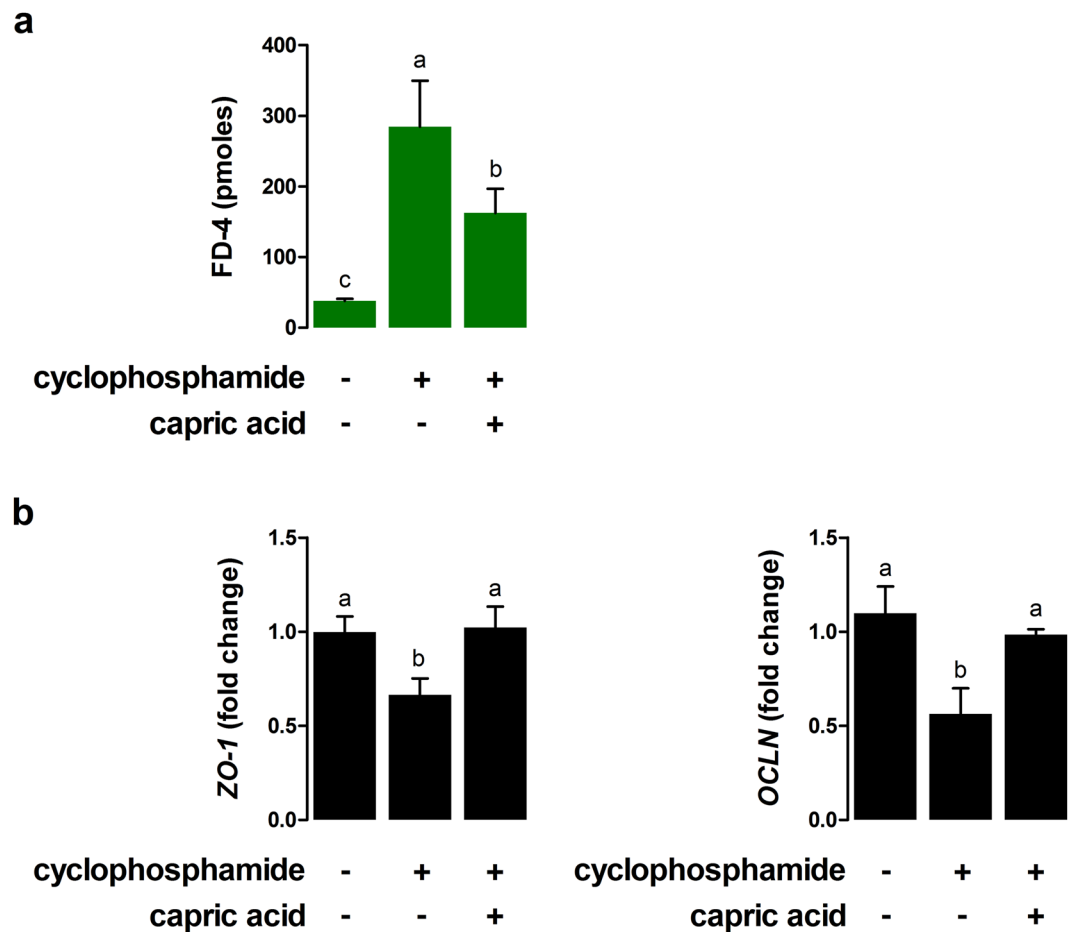


Figure 6. Effects of capric acid treatment on intestinal permeability after cyclophosphamide treatment in IPEC-J2 cells. **(a)** Membrane FD-4 permeability of cyclophosphamide-induced IPEC-J2 cells with or without capric acid pre-treatment. Membrane permeability was quantitated by measuring the amount of FD-4 that permeated the IPEC-J2 monolayer. **(b)** Relative quantitative expression of the genes encoding tight junctions (*ZO-1* and *OCLN*) for capric acid treatment after cyclophosphamide treatment in IPEC-J2 cells. The qRT-PCR data were normalised to the expression of *GAPDH* as an endogenous control gene and calculated using the $2^{-\Delta\Delta C_t}$ method. Error bars indicate the standard error of the mean ($n = 3$). A p-value of <0.05 indicated statistical significance. Lowercase letters (a, b, c) indicate significant differences between treatments based on Duncan multiple range tests.

of general mechanisms. $\text{NF-}\kappa\text{B}$ is a transcription factor involved in the upregulation of inflammatory cytokines including TNFs and ILs²⁶. According to a previous report, capric acid inhibits inflammatory cytokines such as IL-8, IL-6, and TNF- α by the inhibition of MAPK phosphorylation and NF- κB activation²⁴. The authors

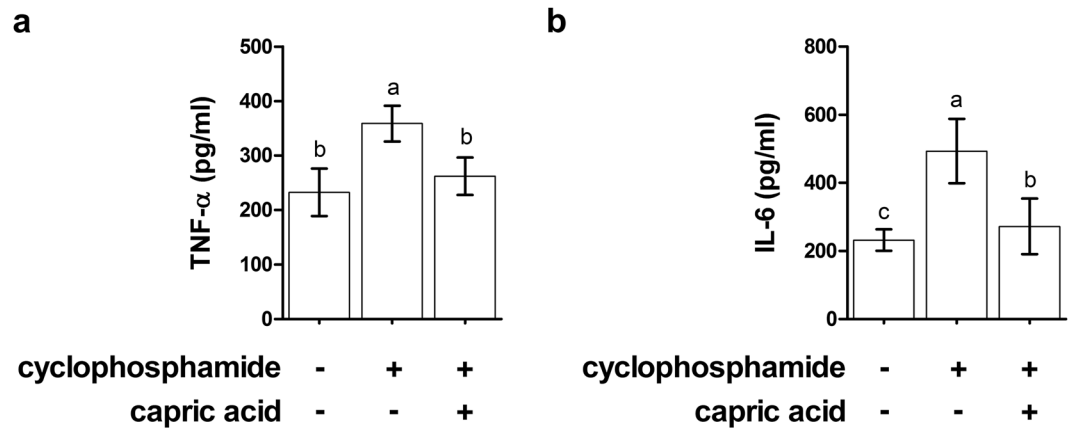


Figure 7. Effects of capric acid on the production of the inflammatory cytokines TNF- α and IL-6 in the blood serum after the CTX challenge. Miniature pigs were randomly allocated into three groups: (T1) control diet + saline challenge; (T2) control diet + CTX challenge; and (T3) control diet with 0.5% capric acid + CTX challenge. Concentrations of TNF- α and IL-6 were determined by ELISA ($n = 5$). Error bars indicate the standard error of the mean ($n = 3$). A p-value of < 0.05 was considered to indicate statistical significance. Lowercase letters (a, b, c) indicate significant differences between treatments based on Duncan multiple range tests.

elucidated the mechanism by which capric acid attenuates cytokine production and reported that capric acid at 100 mM significantly suppresses phosphorylated MAPKs, such as p38, JNK, and ERK, and significantly increased NF- κ B p65 translocation²⁴. Additionally, PPAR- γ is a transcription factor with anti-inflammatory functions. Capric acid can regulate inflammatory gene expression and it interferes with the activation of NF κ B creating an intriguing interaction between these two transcription factors²⁷. A previous report suggested that capric acid is a modulating ligand for PPARs²⁸. They demonstrated that capric acid occupies a novel binding site and only partially stabilizes the AF-2 helix of PPAR α and binds to PPAR α and PPAR β/δ ²⁸. These observations suggest that capric acid influences inflammatory gene expression via the inhibition of the activation of NF κ B and PPARs.

MCFAs occur naturally as medium-chain triglycerides in milk fat and various feed materials; they have specific nutritional effects and can be utilised directly by enterocytes for energy production and thereby support the integrity of the intestine in young piglets²¹. According to a previous report, capric acid enhances IL-8 production in human intestinal epithelial cells (Caco-2), influencing cell function via cellular PKC activity²⁹.

Fatty acids induce porcine host defence peptide gene expression in IPEC-J2 intestinal epithelial cells; they improve intestinal morphology, reduce the total viable counts of proximal colon *Clostridium* and *Escherichia coli*, and decrease TNF- α and IL-6 levels in the serum and DNA-binding activity of intestinal nuclear factor- κ B in pigs³⁰. Taken together, MCFAs, such as capric acid, attenuate intestinal inflammation and promote intestinal health in pigs.

In the present study, capric acid treatment alleviated oxidative stress induced by cyclophosphamide in small intestinal epithelial cells. Management and nutritional strategies have been developed to maximise growth performance and livestock health by considering GI health. The intestinal epithelium plays critical roles in nutrient absorption, the mucosal immune response to pathogenic bacteria, and the regulation of mucosal tissue homeostasis³¹. Because the GI tract comprises more than 70% of the immune cells in the body, the activation of the GI immune system is directly related to livestock health¹. The small intestine is vulnerable to damage induced by toxins, such as pathogens and toxic chemicals, which affect plasma and intracellular ROS production, resulting in apoptosis and reducing antioxidative capacity and mitochondrial dysfunction^{32–34}. The small intestinal epithelial cell is the main target of harmful factors and stress, including toxins and ROS³⁵. The imbalance between ROS and antioxidants induces oxidative stress, resulting in the retardation of growth in livestock³⁶. According to a previous study, MCFA (caprylic, capric, and lauric)-rich rice bran oils ameliorate arsenite-induced oxidative stress in rats³⁷.

The intestinal epithelium has two main functions, i.e. the traffic of nutrients from the lumen and the restriction of the passage of potentially harmful microorganisms and toxins as an intestinal epithelial barrier or paracellular permeability mechanism^{38,39}. In the present study, we focused on the epithelial barrier function of capric acid. To maintain the epithelial barrier, effective intercellular junctions are important. Paracellular permeability of harmful microorganisms and toxins is regulated primarily by epithelial intercellular junctions, such as the tight junctions, adherens junctions, and desmosomes⁴⁰. Among epithelial intercellular junctions, adherens junctions and desmosomes are critical for the maintenance of the proximity between epithelial cells via intercellular molecular connections, whereas tight junctions play a role in sealing the paracellular space⁴¹. In the present study, cyclophosphamide increased the permeability of fluorescent dextran (40 kDa), whereas capric acid treatment restored impaired epithelial barrier function in small intestinal epithelial cells. Additionally, capric acid treatment increased the expression of tight junction-related genes, such as *ZO-1* and *OCN1*, which decreased in response to cyclophosphamide treatment⁴². In agreement with the results of this study, nutrients, such as butyrate, amino acids, and vitamins, play critical roles in intestinal permeability and integrity, as well in the paracellular permeability responsible for allowing the absorption of nutrients and other macromolecules^{43–45}. These findings suggested

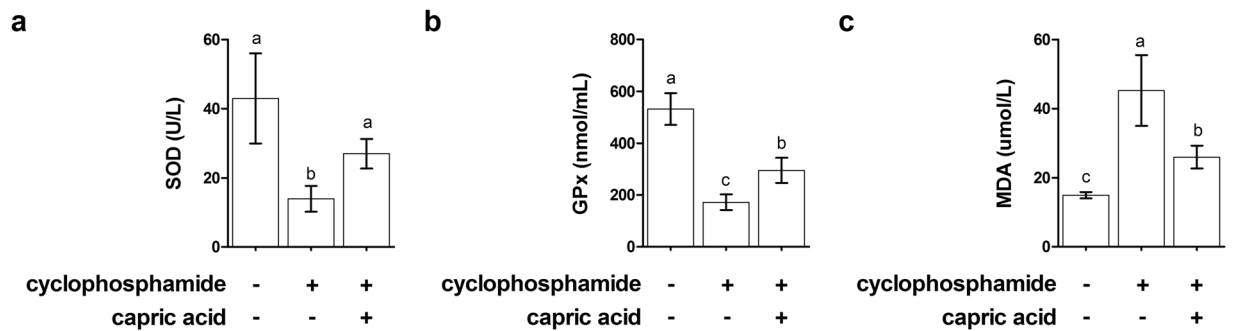


Figure 8. Effects of capric acid on SOD (a), GPx (b), and MDA (c) levels in the blood serum after the CTX challenge. Miniature pigs were randomly allocated into three groups: (T1) control diet + saline challenge; (T2) control diet + CTX challenge; and (T3) control diet with 0.5% capric acid + CTX challenge. Concentrations of SOD, GPx, and MDA were determined by ELISA ($n = 5$). Error bars indicate the standard error of the mean ($n = 3$). A p -value of < 0.05 was considered to indicate statistical significance. Lowercase letters (a, b, c) indicate significant differences between treatments based on Duncan multiple range tests.

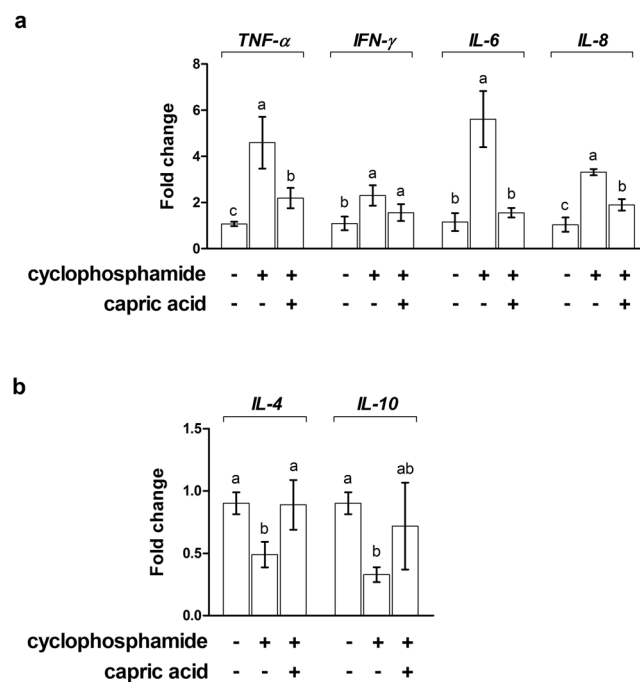


Figure 9. Relative quantitative expression of genes encoding (a) pro-inflammatory cytokines (TNF- α , IFN- γ , and IL-6) and (b) anti-inflammatory cytokines (IL-4 and IL-10) for capric acid treatment after cyclophosphamide challenge in peripheral blood mononuclear cells of miniature pigs. Miniature pigs were randomly allocated into three groups: (T1) control diet + saline challenge; (T2) control diet + CTX challenge; and (T3) control diet with 0.5% capric acid + CTX challenge. The qRT-PCR data were normalised relative to the expression of *GAPDH* as an endogenous control gene and calculated using the $2^{-\Delta\Delta C_t}$ method. Error bars indicate the standard error of the mean. A p -value of < 0.05 was considered to indicate statistical significance. Lowercase letters (a, b, c) indicate significant differences between treatments based on Duncan multiple range tests.

that crosstalk between nutrients and epithelial barrier function occurred by the dynamic regulation of the tight junction and enhance intestinal barrier function via nutritional manipulation.

The pig is a major animal model used in nutritional and translational research and is an alternative to the dog or monkey as a non-rodent animal model in the toxicological testing of pharmaceuticals⁴⁶. In the present study, we investigated the functions of capric acid in cyclophosphamide-treated small intestinal epithelial cells *in vitro* and used miniature pigs as a non-rodent animal model to investigate the function of capric acid in the small intestine. Both humans and minipigs are omnivores and accordingly have similarities with respect to the physiological function of the GI system^{46,47}. The small intestinal system of minipigs offers some anatomical and functional advantages, such as absorption and metabolism, compared to other non-rodent animal models for *in vivo* testing. In the present study, 0.5% capric acid was used, which is much higher than the amount used in a previous study

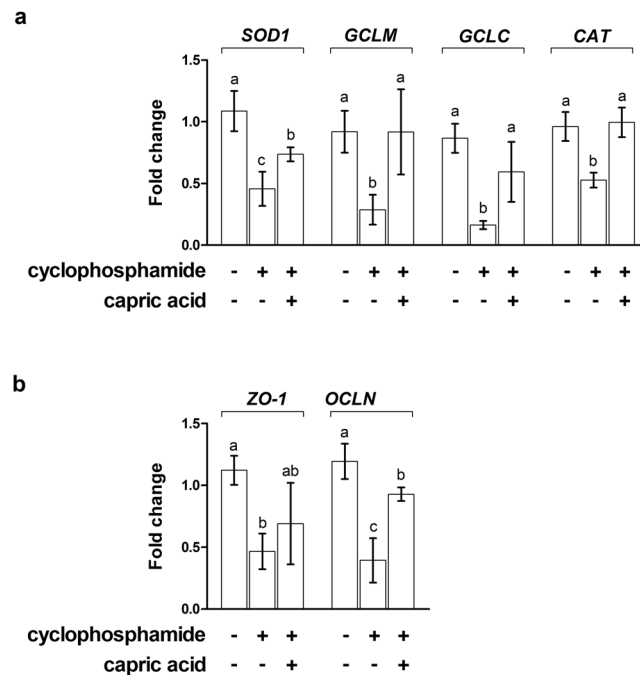


Figure 10. Relative quantitative expression of genes encoding (a) antioxidant enzymes (SOD1, GCLM, GCLC, and CAT) and (b) tight junctions (ZO-1 and OCLN) after capric acid treatment and cyclophosphamide challenge in peripheral blood mononuclear cells of miniature pigs. The miniature pigs were randomly allocated into three groups: (T1) control diet + saline challenge; (T2) control diet + CTX challenge; and (T3) control diet with 0.5% capric acid + CTX challenge. The qRT-PCR data were normalised relative to the expression of *GAPDH* as an endogenous control gene and calculated using the $2^{-\Delta\Delta C_t}$ method. Error bars indicate the standard error of the mean. A p-value of <0.05 was considered to indicate statistical significance. Lowercase letters (a,b,c) indicate significant differences between treatments based on Duncan multiple range tests.

(0.2% capric acid) showing a dramatic effect of capric acid *in vivo*²⁵. The previous study reported that 0.2% capric acid supplementation improved piglet performance and the structure of the ileum²⁵. Therefore, to determine the appropriate dose of capric acid *in vivo*, further analyses are needed.

In conclusion, it has been reported that MCFAs support the integrity of the intestine, increasing the length of villi and reducing the crypt depth in the small intestine. However, owing to differences in the effects of each MCFA, it is important to study the effect on each fatty acid, such as capric acid, on the intestinal epithelium and the integrity of the intestine. Therefore, in the present study, the effects of a MCFA, capric acid, on intestinal oxidative stress, inflammation, and barrier function were examined in porcine epithelial cells and miniature pigs after treatment with the immune suppressant cyclophosphamide. Capric acid alleviated inflammatory cytokine production (TNF- α and IL-6) and related gene expression (*NF- κ B*, *TNF- α* , *IFN- γ*), alleviated oxidative stress (GSSG/GSH ratio, H_2O_2 , and malondialdehyde), and increased oxidative stress-related gene expression (*SOD1* and *GCLC*) in cyclophosphamide-treated IPEC-J2 cells. Furthermore, the permeability of FD-4 and expression of *ZO-1* and *OCLN* in cyclophosphamide-treated IPEC-J2 cells were reduced by capric acid. Furthermore, dietary capric acid reduced TNF- α , IL-6, and MDA levels and increased SOD, GPx, and the expression of genes related to pro-inflammatory, oxidative stress, and intestinal barrier functions in cyclophosphamide-treated miniature pigs. Our results demonstrated that capric acid improves protection against cyclophosphamide-induced intestinal inflammation, oxidative stress, and barrier function in porcine small intestinal epithelial cells *in vitro* and miniature pigs *in vivo*. Our data improve our general understanding of the functions of capric acid in the small intestine of pigs.

Methods

Cell line and culture conditions. The non-transformed porcine intestinal epithelial cell line (IPEC-J2; DSMZ, Braunschweig, Germany), originally isolated from jejunal epithelia of a neonatal unsuckled piglet, were cultured in Dulbecco's modified Eagle medium (DMEM) and Ham's F-12 medium mixed at a 1:1 ratio (Gibco Life Technologies, Grand Island, NY, USA) supplemented with 5% foetal bovine serum, 1% insulin-transferrin-selenium-X, and 1% (v/v) penicillin-streptomycin mixture⁴⁸. Cells were grown at 37 °C in a humidified atmosphere of 5% CO₂.

IPEC-J2 cells were incubated with various concentrations of capric acid (Sigma–Aldrich, Seoul, Korea) for 24 h before cyclophosphamide induction. For cyclophosphamide induction, the IPEC-J2 cells were incubated with various concentrations of cyclophosphamide for 1 h. Cyclophosphamide was removed by washing twice with PBS.

Analyses of TNF- α , IL-6, GSSG/GSH ratio, intracellular H₂O₂, and malondialdehyde levels *in vitro*. After 1 h of treatment with cyclophosphamide, IPEC-J2 cells were incubated with fresh cell culture medium. Culture media were collected after 12 h. The samples were centrifuged (245 \times g, 10 min) and cytokine concentrations were measured. The levels of TNF- α , IL-6, and malondialdehyde secretion were determined using Porcine-specific Enzyme-linked Immunosorbent Assay (ELISA) Kits (Thermo Scientific, Waltham, MA, USA) according to the manufacturer's instructions.

To measure the GSSG/GSH ratio, IPEC-J2 cells were pre-treated with or without capric acid for 24 h followed by cyclophosphamide treatment for 1 h using the GSH/GSSG-Glo Glutathione Assay (Promega, Madison, WI, USA). Cells cultured in a 96-well culture plate were harvested after 24 h of treatment by the removal of the cell culture medium, followed by immediate lysis and assays for total and oxidised GSH, following the manufacturer's instruction.

To measure ROS, the level of intracellular H₂O₂ was analysed using the Amplex Red Hydrogen Peroxide Assay Kit (Invitrogen, Molecular Probes, Eugene, OR, USA). IPEC-J2 cells were pre-treated with or without capric acid for 24 h, followed by cyclophosphamide treatment for 1 h in phenol red-free DMEM. The H₂O₂ concentrations in the medium were determined using the working solution of 100 μ M Amplex Red reagent and 0.2 U/mL horseradish peroxidase. H₂O₂ determination was also performed. After 60 min of incubation with the dye at 25 °C H₂O₂ was quantitatively analysed; the excitation wavelength was set at 560 nm and emission was measured at 590 nm (Victor \times 2 2030 Fluorometer; Perkin Elmer, Waltham, MA, USA).

Permeability assay. When the IPEC-J2 monolayer was confluent (≥ 1 k Ω cm²), the cells were treated with or without capric acid for 24 h. The cells were washed twice and incubated with cyclophosphamide for 1 h. The cells were washed twice again. The permeability assay started when 500 μ L of culture medium containing 50 μ g of FD-4 (Sigma-Aldrich) was added to the apical chamber. The basolateral chamber was filled with 1.5 mL of culture medium (37 °C, 5% CO₂). FD-4 was allowed to permeate overnight (18 h) from the apical to the basolateral chamber. Subsequently, 100 μ L of the basolateral chamber medium was transferred to a 96-well plate to measure the amount of permeated FD-4 using a flour-spectrophotometer (Ex/Em: 490/520 nm).

***In vivo* cyclophosphamide challenge in pigs.** All experiments were approved by the Animal Care Committee of Dankook University and were conducted in accordance with the guidelines for the care and use of experimental animals for research at Dankook University. A total of 15 miniature pigs [MK strain, (Duroc \times Yorkshire) \times (Pot Valley \times Berkshire) \times Yucatan] with an average initial body weight of 20.92 \pm 0.24 kg were used to evaluate the effects of dietary capric acid over a 21-day period. Each pig was kept in an individual pen and housed in an environmentally controlled nursery facility with slatted plastic flooring and a mechanical ventilation system. Each room was maintained at approximately 27 °C and 60% humidity. Each pen was equipped with a one-sided, stainless steel self-feeder and a nipple drinker, which allowed *ad libitum* access to feed and water. Experimental treatments were as follows: (T1) control diet + saline challenge, (T2) control diet + CTX challenge, and (T3) control diet with 0.5% capric acid + CTX challenge. The control diet was based on corn and soybean meal.

For the CTX challenge assay, all pigs from each dietary treatment group were injected intraperitoneally with CTX or a saline solution at day 14. CTX (Sigma-Aldrich) was diluted in a sterile saline solution and injected at 0.01% (50 mg/kg) of the body weight on the 14th day after the feeding trial. The dose of CTX was determined based on the results of a previous study⁴⁹. No vaccines or antibiotics were used in this experiment.

Blood collection and biochemical analysis. At the end of the experiment (21st day), blood samples were collected and analysed according to our standard protocol⁵⁰. Briefly, blood samples were collected from all pigs via jugular venipuncture 6 h after the challenge into a non-heparinised K₃EDTA vacuum tube (Becton Dickinson Vacutainer Systems, Franklin Lakes, NJ, USA) to obtain serum and whole blood. Leukocyte, lymphocyte, and monocyte counts were determined using an automatic blood analyser (ADVIA 120; Bayer, Leverkusen, Germany).

The whole blood samples were subsequently centrifuged at 3,000 \times g for 15 min at 4 °C, and the serum was harvested. Thereafter, the samples were frozen and stored at -20 °C until further analysis. The levels of serum TNF- α (R&D Systems, Minneapolis, MN, USA), IL-6 (R&D Systems), superoxide dismutase (SOD) (Cohesion Biosciences, London, UK), glutathione peroxidase (GPx) (Cayman Chemical, Ann Arbor, MI, USA), and malondialdehyde (MDA) (Abcam, Cambridge, UK) were determined using an ELISA kit.

Peripheral blood mononuclear cell preparation. For PBMC isolation, blood samples (5–10 mL) from 15 pigs were collected in a K₃EDTA vacuum tube at the end of the experiment. PBMCs were prepared according to a previous study⁵¹. Briefly, the collected blood samples were diluted with an equal volume of a balanced salt solution, and PBMCs were immediately isolated by Histopaque density gradient centrifugation according to the manufacturer's instructions (Sigma-Aldrich). Briefly, the diluted blood samples were mixed with a half volume of a Histopaque solution and then centrifuged at 400 \times g for 35 min at room temperature. PBMCs were carefully aspirated from the Histopaque solution–plasma interface.

Quantitative real-time polymerase chain reaction. RNA was isolated using TRIzol reagent (Invitrogen, Carlsbad, CA, USA). For quantitative real-time polymerase chain reaction (RT-qPCR), total RNA (0.1–1 μ g) was used for complementary DNA synthesis using the Maxima First-strand cDNA Synthesis Kit (Life Technologies). The primers for RT-qPCR for each gene transcript were designed using Primer3 (<http://frodo.wi.mit.edu/>) (Table 1). RT-qPCR was performed using a 7500 Fast Real-time PCR System (Applied Biosystems). The RT-qPCR conditions were as follows: 94 °C for 3 min, followed by 40 cycles at 94 °C for 30 s, 59–61 °C for 30 s,

Gene symbol	Description	Accession No.	Forward (5' → 3')	Reverse (5' → 3')
<i>TNF-α</i>	Tumor necrosis factor alpha	NM_214022	TCTCCTTCCTCCTGGTCGCA	TCCCTCGGCTTTGACATTGG
<i>IFN-γ</i>	Interferon gamma	NM_213948	GGCCATTCAAAGGAGCATGG	GATGGCTTTGCGCTGGATCT
<i>NF-κB</i>	Nuclear factor of kappa light polypeptide gene enhancer in B-cells 1	NM_001048232	GACAACATCTCCTTGGCGGG	TCTGCTCCTGCTGCTTTGAGG
<i>IL-4</i>	Interleukin-4	NM_214123	TCCACGGACACAAGTGCGAC	TGTTTGGCATGCTGCTCAGG
<i>IL-6</i>	Interleukin-6	NM_214399	AGCCCACCAGGAACGAAAGA	AGCCATACCAGAAGCAGCC
<i>IL-10</i>	Interleukin-10	NM_214041	CATCCACTTCCCAACCAGCC	CTCCCCATCACTCTCTGCCTTC
<i>SOD1</i>	Superoxide dismutase 1	NM_001190422	GTACCAGTGCAGGTCCTCAC	TTTGCCAGCAGTCACATTGC
<i>GCLM</i>	Glutamate-cysteine ligase modifier subunit	XM_001926378	TTGGAGCAGCTGTACCAGTG	GAGTTCCTGGAAACTCGCT
<i>GCLC</i>	Glutamate-cysteine ligase catalytic subunit	XM_003482164	GTCCAGTTGGTCTCTGTCTGG	CGGGAGTCCCTTCGATCATG
<i>CAT</i>	Catalase	NM_214301	ACACAGGCACATGAACGGAT	GTCCCGGATGCCATAGTCAG
<i>ZO-1</i>	Zonula occludens 1	XM_021098856	GATCCTGACCCGGTGTCTGA	TTGGTGGGTTTGGTGGGTTG
<i>OCN</i>	Occludin	NM_001163647	GAGAGAGTGGACAGCCCAT	TGCTGTGTAATGAGGCTGC
<i>GAPDH</i>	Glyceraldehyde-3-phosphate dehydrogenase	NM_001206359	AATGGGGTGATGCTGGTGCT	GGCAGAAGGGGCAGAGATGA

Table 1. List of primers.

and 72 °C for 30 s. Melting curve profiles were analysed for the amplicons. RT-qPCR data were normalised relative to the expression of glyceraldehyde 3-phosphate dehydrogenase (*GAPDH*), an endogenous control gene, and calculated using the $2^{-\Delta\Delta Ct}$ method, where $\Delta\Delta Ct$ (cycle threshold) = ΔCt (treated) – ΔCt (control) and $\Delta Ct = Ct$ of the target gene – Ct of *GAPDH* (treated or control, respectively)⁵².

Statistical analysis. Data were analysed with the general linear model (PROC-GLM) procedure of SAS to determine the significance of differences between the treatments. Results are presented as means and the standard error of the mean ($n \geq 3$, where n refers to the number of replicate experiments). The individual miniature pigs were considered the experimental unit. A p -value of < 0.05 indicated statistical significance. Significant differences between treatments were assessed by Duncan multiple range tests.

References

- Blikslager, A. T., Moeser, A. J., Gookin, J. L., Jones, S. L. & Odle, J. Restoration of barrier function in injured intestinal mucosa. *Physiological reviews* **87**, 545–564, <https://doi.org/10.1152/physrev.00012.2006> (2007).
- Liu, Y. *et al.* Fish oil enhances intestinal integrity and inhibits TLR4 and NOD2 signaling pathways in weaned pigs after LPS challenge. *The Journal of nutrition* **142**, 2017–2024, <https://doi.org/10.3945/jn.112.164947> (2012).
- Pie, S. *et al.* Weaning is associated with an upregulation of expression of inflammatory cytokines in the intestine of piglets. *The Journal of nutrition* **134**, 641–647 (2004).
- Yi, G. F. *et al.* Effect of glutamine and spray-dried plasma on growth performance, small intestinal morphology, and immune responses of Escherichia coli K88+ -challenged weaned pigs. *Journal of animal science* **83**, 634–643 (2005).
- Lee, J. S. *et al.* Effect of Lactobacillus plantarum CJLP243 on the growth performance and cytokine response of weaning pigs challenged with enterotoxigenic Escherichia coli. *Journal of animal science* **90**, 3709–3717, <https://doi.org/10.2527/jas.2011-4434> (2012).
- Willing, B. P. & Van Kessel, A. G. Intestinal microbiota differentially affect brush border enzyme activity and gene expression in the neonatal gnotobiotic pig. *Journal of animal physiology and animal nutrition* **93**, 586–595, <https://doi.org/10.1111/j.1439-0396.2008.00841.x> (2009).
- Camilleri, M., Madsen, K., Spiller, R., Greenwood-Van Meerveld, B. & Verne, G. N. Intestinal barrier function in health and gastrointestinal disease. *Neurogastroenterology and motility: the official journal of the European Gastrointestinal Motility Society* **24**, 503–512, <https://doi.org/10.1111/j.1365-2982.2012.01921.x> (2012).
- Liu, Y. Fatty acids, inflammation and intestinal health in pigs. *Journal of animal science and biotechnology* **6**, 41, <https://doi.org/10.1186/s40104-015-0040-1> (2015).
- Nathan, C. & Cunningham-Bussel, A. Beyond oxidative stress: an immunologist's guide to reactive oxygen species. *Nature reviews. Immunology* **13**, 349–361, <https://doi.org/10.1038/nri3423> (2013).
- Bhattacharyya, A., Chattopadhyay, R., Mitra, S. & Crowe, S. E. Oxidative stress: an essential factor in the pathogenesis of gastrointestinal mucosal diseases. *Physiological reviews* **94**, 329–354, <https://doi.org/10.1152/physrev.00040.2012> (2014).
- John, L. J., Fromm, M. & Schulzke, J. D. Epithelial barriers in intestinal inflammation. *Antioxidants & redox signaling* **15**, 1255–1270, <https://doi.org/10.1089/ars.2011.3892> (2011).
- Rezaie, A., Parker, R. D. & Abdollahi, M. Oxidative stress and pathogenesis of inflammatory bowel disease: an epiphenomenon or the cause? *Digestive diseases and sciences* **52**, 2015–2021, <https://doi.org/10.1007/s10620-006-9622-2> (2007).
- Rao, R. K. *et al.* Tyrosine phosphorylation and dissociation of occludin-ZO-1 and E-cadherin-beta-catenin complexes from the cytoskeleton by oxidative stress. *The Biochemical journal* **368**, 471–481, <https://doi.org/10.1042/BJ20011804> (2002).
- Rao, R. K., Baker, R. D., Baker, S. S., Gupta, A. & Holycross, M. Oxidant-induced disruption of intestinal epithelial barrier function: role of protein tyrosine phosphorylation. *The American journal of physiology* **273**, G812–G823 (1997).
- Rao, R., Baker, R. D. & Baker, S. S. Inhibition of oxidant-induced barrier disruption and protein tyrosine phosphorylation in Caco-2 cell monolayers by epidermal growth factor. *Biochemical pharmacology* **57**, 685–695 (1999).
- Geens, M. M. & Niewold, T. A. Optimizing culture conditions of a porcine epithelial cell line IPEC-J2 through a histological and physiological characterization. *Cytotechnology* **63**, 415–423, <https://doi.org/10.1007/s10616-011-9362-9> (2011).
- Lewis, K. *et al.* Enhanced translocation of bacteria across metabolically stressed epithelia is reduced by butyrate. *Inflammatory bowel diseases* **16**, 1138–1148, <https://doi.org/10.1002/ibd.21177> (2010).
- Wang, N. *et al.* Curcumin ameliorates hydrogen peroxide-induced epithelial barrier disruption by upregulating heme oxygenase-1 expression in human intestinal epithelial cells. *Digestive diseases and sciences* **57**, 1792–1801, <https://doi.org/10.1007/s10620-012-2094-7> (2012).

19. Calder, P. C. Fatty acids and inflammation: the cutting edge between food and pharma. *European journal of pharmacology* **668**(Suppl 1), S50–58, <https://doi.org/10.1016/j.ejphar.2011.05.085> (2011).
20. Odle, J. New insights into the utilization of medium-chain triglycerides by the neonate: observations from a piglet model. *The Journal of nutrition* **127**, 1061–1067 (1997).
21. Guillot, E., Vaugelade, P., Lemarchal, P. & Rerat, A. Intestinal absorption and liver uptake of medium-chain fatty acids in non-anaesthetized pigs. *The British journal of nutrition* **69**, 431–442 (1993).
22. Dierick, N., Michiels, J. & Van Nevel, C. Effect of medium chain fatty acids and benzoic acid, as alternatives for antibiotics, on growth and some gut parameters in piglets. *Communications in agricultural and applied biological sciences* **69**, 187–190 (2004).
23. Ferrara, F., Tedin, L., Pieper, R., Meyer, W. & Zentek, J. Influence of medium-chain fatty acids and short-chain organic acids on jejunal morphology and intra-epithelial immune cells in weaned piglets. *Journal of animal physiology and animal nutrition* **101**, 531–540, <https://doi.org/10.1111/jpn.12490> (2017).
24. Huang, W. C. *et al.* Anti-bacterial and anti-inflammatory properties of capric acid against *Propionibacterium acnes*: a comparative study with lauric acid. *Journal of dermatological science* **73**, 232–240, <https://doi.org/10.1016/j.jderm.2013.10.010> (2014).
25. Hanczakowska, E., Szcwyczyk, A. & Okon, K. Effects of dietary caprylic and capric acids on piglet performance and mucosal epithelium structure of the ileum. *J Anim Feed Sci* **20**, 556–565 (2011).
26. Kremer, J. M. *et al.* Dietary fish oil and olive oil supplementation in patients with rheumatoid arthritis. *Clinical and immunologic effects. Arthritis and rheumatism* **33**, 810–820 (1990).
27. Vanden Berghe, W. *et al.* A paradigm for gene regulation: inflammation, NF-kappaB and PPAR. *Advances in experimental medicine and biology* **544**, 181–196 (2003).
28. Malapaka, R. R. *et al.* Identification and mechanism of 10-carbon fatty acid as modulating ligand of peroxisome proliferator-activated receptors. *The Journal of biological chemistry* **287**, 183–195, <https://doi.org/10.1074/jbc.M111.294785> (2012).
29. Tanaka, S. *et al.* Medium-chain fatty acids stimulate interleukin-8 production in Caco-2 cells with different mechanisms from long-chain fatty acids. *Journal of gastroenterology and hepatology* **16**, 748–754 (2001).
30. Zeng, X. *et al.* Induction of porcine host defense peptide gene expression by short-chain fatty acids and their analogs. *PLoS one* **8**, e72922, <https://doi.org/10.1371/journal.pone.0072922> (2013).
31. Haller, D. *et al.* Non-pathogenic bacteria elicit a differential cytokine response by intestinal epithelial cell/leucocyte co-cultures. *Gut* **47**, 79–87 (2000).
32. Xiao, H. *et al.* Effects of composite antimicrobial peptides in weanling piglets challenged with deoxynivalenol: I. Growth performance, immune function, and antioxidation capacity. *Journal of animal science* **91**, 4772–4780, <https://doi.org/10.2527/jas.2013-6426> (2013).
33. Xiao, H. *et al.* Effects of composite antimicrobial peptides in weanling piglets challenged with deoxynivalenol: II. Intestinal morphology and function. *Journal of animal science* **91**, 4750–4756, <https://doi.org/10.2527/jas.2013-6427> (2013).
34. Tan, B. *et al.* L-arginine improves DNA synthesis in LPS-challenged enterocytes. *Front Biosci (Landmark Ed)* **20**, 989–1003 (2015).
35. Vandenbroucke, V. *et al.* The mycotoxin deoxynivalenol potentiates intestinal inflammation by *Salmonella typhimurium* in porcine ileal loops. *PLoS one* **6**, e23871, <https://doi.org/10.1371/journal.pone.0023871> (2011).
36. Yin, J. *et al.* Effects of dietary supplementation with glutamate and aspartate on diquat-induced oxidative stress in piglets. *PLoS one* **10**, e0122893, <https://doi.org/10.1371/journal.pone.0122893> (2015).
37. Sengupta, A., Ghosh, M. & Bhattacharyya, D. K. Antioxidative effect of rice bran oil and medium chain fatty acid rich rice bran oil in arsenite induced oxidative stress in rats. *Journal of oleo science* **63**, 1117–1124 (2014).
38. Barrett, K. E. Epithelial biology in the gastrointestinal system: insights into normal physiology and disease pathogenesis. *The Journal of physiology* **590**, 419–420, <https://doi.org/10.1113/jphysiol.2011.227058> (2012).
39. Koch, S. & Nusrat, A. The life and death of epithelia during inflammation: lessons learned from the gut. *Annual review of pathology* **7**, 35–60, <https://doi.org/10.1146/annurev-pathol-011811-120905> (2012).
40. Giepmans, B. N. & van Ijzendoorn, S. C. Epithelial cell-cell junctions and plasma membrane domains. *Biochimica et biophysica acta* **1788**, 820–831, <https://doi.org/10.1016/j.bbame.2008.07.015> (2009).
41. Manresa, M. C. & Taylor, C. T. Hypoxia Inducible Factor (HIF) Hydroxylases as Regulators of Intestinal Epithelial Barrier Function. *Cellular and molecular gastroenterology and hepatology* **3**, 303–315, <https://doi.org/10.1016/j.jcmgh.2017.02.004> (2017).
42. Gunzel, D. & Yu, A. S. Claudins and the modulation of tight junction permeability. *Physiological reviews* **93**, 525–569, <https://doi.org/10.1152/physrev.00019.2012> (2013).
43. Cunningham, K. E. & Turner, J. R. Myosin light chain kinase: pulling the strings of epithelial tight junction function. *Annals of the New York Academy of Sciences* **1258**, 34–42, <https://doi.org/10.1111/j.1749-6632.2012.06526.x> (2012).
44. Ballard, S. T., Hunter, J. H. & Taylor, A. E. Regulation of tight-junction permeability during nutrient absorption across the intestinal epithelium. *Annual review of nutrition* **15**, 35–55, <https://doi.org/10.1146/annurev.nu.15.070195.000343> (1995).
45. Amasheh, M., Andres, S., Amasheh, S., Fromm, M. & Schulzke, J. D. Barrier effects of nutritional factors. *Annals of the New York Academy of Sciences* **1165**, 267–273, <https://doi.org/10.1111/j.1749-6632.2009.04063.x> (2009).
46. Swindle, M. M. *et al.* Swine as models in biomedical research and toxicology testing. *Veterinary pathology* **49**, 344–356, <https://doi.org/10.1177/0300985811402846> (2012).
47. Bode, G. *et al.* The utility of the minipig as an animal model in regulatory toxicology. *Journal of pharmacological and toxicological methods* **62**, 196–220, <https://doi.org/10.1016/j.vascn.2010.05.009> (2010).
48. Schierack, P. *et al.* Characterization of a porcine intestinal epithelial cell line for *in vitro* studies of microbial pathogenesis in swine. *Histochemistry and cell biology* **125**, 293–305, <https://doi.org/10.1007/s00418-005-0067-z> (2006).
49. Han, J. *et al.* Dietary L-arginine supplementation alleviates immunosuppression induced by cyclophosphamide in weaned pigs. *Amino acids* **37**, 643–651, <https://doi.org/10.1007/s00726-008-0184-9> (2009).
50. Li, J. & Kim, I. H. Effects of levan-type fructan supplementation on growth performance, digestibility, blood profile, fecal microbiota, and immune responses after lipopolysaccharide challenge in growing pigs. *Journal of Animal Science* **91**, 5336–5343, <https://doi.org/10.2527/jas.2013-6665> (2013).
51. Lee, S. I., Kim, H. S., Koo, J. M. & Kim, I. H. *Lactobacillus acidophilus* modulates inflammatory activity by regulating the TLR4 and NF-kappaB expression in porcine peripheral blood mononuclear cells after lipopolysaccharide challenge. *The British journal of nutrition* **115**, 567–575, <https://doi.org/10.1017/S0007114515004857> (2016).
52. Livak, K. J. & Schmittgen, T. D. Analysis of relative gene expression data using real-time quantitative PCR and the 2^{-Delta Delta} C(T) Method. *Methods* **25**, 402–408, <https://doi.org/10.1006/meth.2001.1262> (2001).

Acknowledgements

This work was supported by a grant from the Next-Generation BioGreen 21 Program (Project No. PJ01111504), Rural Development Administration, Republic of Korea.

Author Contributions

S.I.L. designed/supervised the study, carried out the experiments, analysed and interpreted data, and wrote the main manuscript; K.S.K. designed/supervised the study and wrote the manuscript.

Additional Information

Competing Interests: The authors declare that they have no competing interests.

Publisher's note: Springer Nature remains neutral with regard to jurisdictional claims in published maps and institutional affiliations.



Open Access This article is licensed under a Creative Commons Attribution 4.0 International License, which permits use, sharing, adaptation, distribution and reproduction in any medium or format, as long as you give appropriate credit to the original author(s) and the source, provide a link to the Creative Commons license, and indicate if changes were made. The images or other third party material in this article are included in the article's Creative Commons license, unless indicated otherwise in a credit line to the material. If material is not included in the article's Creative Commons license and your intended use is not permitted by statutory regulation or exceeds the permitted use, you will need to obtain permission directly from the copyright holder. To view a copy of this license, visit <http://creativecommons.org/licenses/by/4.0/>.

© The Author(s) 2017